

Research Paper

Aldehyde dehydrogenase 2 protects against oxidative stress associated with pulmonary arterial hypertension

Tao Xu^{a,*}, Shuangyue Liu^{b,1}, Tingting Ma^b, Ziyi Jia^c, Zhifei Zhang^d, Aimei Wang^{b,*}^a Life Science Institute, Jinzhou Medical University, Jinzhou, Liaoning 121000, PR China^b Department of Physiology, Jinzhou Medical University, Jinzhou, Liaoning 121000, PR China^c College of Economics and Management, Huazhong Agricultural University, Wuhan, Hubei 430070, PR China^d Department of Physiology and Pathophysiology, Capital Medical University, School of Basic Medical Sciences, Beijing 100069, PR China

ARTICLE INFO

Keywords:

Pulmonary arterial hypertension
4-hydroxynonenal
Aldehyde dehydrogenase 2
Oxidative stress
NF-κB
Alda-1

ABSTRACT

The cardioprotective benefits of aldehyde dehydrogenase 2 (ALDH2) are well established, although the regulatory role of ALDH2 in vascular remodeling in pulmonary arterial hypertension (PAH) is largely unknown. ALDH2 potently regulates the metabolism of aldehydes such as 4-hydroxynonenal (4-HNE), the endogenous product of lipid peroxidation. Thus, we hypothesized that ALDH2 ameliorates the proliferation and migration of human pulmonary artery smooth muscle cells (HPASMCs) by inhibiting 4-HNE accumulation and regulating downstream signaling pathways, thereby ameliorating pulmonary vascular remodeling. We found that low concentrations of 4-HNE (0.1 and 1 μM) stimulated cell proliferation by enhancing cyclin D1 and c-Myc expression in primary HPASMCs. Low 4-HNE concentrations also enhanced cell migration by activating the nuclear factor kappa B (NF-κB) signaling pathway, thereby regulating matrix metalloproteinase (MMP)-9 and MMP2 expression *in vitro*. *In vivo*, Alda-1, an ALDH2 agonist, significantly stimulated ALDH2 activity, reducing elevated 4-HNE and malondialdehyde levels and right ventricular systolic pressure in a monocrotaline-induced PAH animal model to the level of control animals. Our findings indicate that 4-HNE plays an important role in the abnormal proliferation and migration of HPASMCs, and that ALDH2 activation can attenuate 4-HNE-induced PASMC proliferation and migration, possibly by regulating NF-κB activation, in turn ameliorating vascular remodeling in PAH. This mechanism might reflect a new molecular target for treating PAH.

1. Introduction

Pulmonary arterial hypertension (PAH) is a serious and fatal clinical syndrome characterized by pulmonary vascular remodeling, which leads to a mean pulmonary artery pressure above 25 mm Hg, right ventricular failure, and death [1]. PAH is a multi-factorial process with a very complex pathological mechanism. Abnormal proliferation of the pulmonary arterial smooth muscle cells (PASMCs) typically underpins its pathology [2,3]. In recent years, extensive studies in both animal models and patients suggested that oxidative stress plays a key role in pathological remodeling of the pulmonary vasculature [4]. Excessive lipid peroxidation participates in the abnormal proliferation of PASMCs [5].

4-hydroxynonenal (HNE) is a major end product of lipid peroxidation, derived from the oxidation of *n*-6 polyunsaturated fatty acids, such as linoleic, γ-linolenic, or arachidonic acids [6]. 4-HNE is not only

a marker of oxidative stress, but can also form protein adducts and dysregulate cell signaling to contribute to multiple diseases, including cancer, atherosclerosis, and hypertension [7–9]. 4-HNE has been reported to stimulate the proliferation of vascular smooth muscle cells [10–12]. The accumulation of 4-HNE in the pulmonary arteries in patients with PAH has been recognized as an important contributor to disease progression [13,14]; however, the role of 4-HNE in the abnormal proliferation of pulmonary vascular smooth muscle cells, and the associated signaling pathways involved remain unknown.

Aldehyde dehydrogenase (ALDH) 2 is a key enzyme mediating the conversion of aldehydes, e.g., 4-HNE, into much less reactive chemical species [15]. Previous data have indicated that ALDH2 activity is closely associated with several cellular functions, including proliferation and responses to oxidative stress [16]. The *ALDH2* gene is linked to susceptibility to cardiovascular diseases [17,18]. Polymorphism of the *ALDH2* gene is implicated in inflammatory processes associated

* Corresponding authors.

E-mail addresses: 5xu5_888@163.com (T. Xu), aimeiwang@lnmu.edu.cn (A. Wang).¹ These authors contributed equally to this work.

with coronary heart disease and hypertension [19,20]. Although the exact role of ALDH2 in pulmonary vascular remodeling is unknown, it is very likely that ALDH2 contributes to the development and progression of PAH. In this study, we investigated whether 4-NHE accumulation was responsible for the abnormal proliferation and migration of pulmonary vascular smooth muscle cells, and whether Alda-1 (an ALDH2 agonist) affects perfusion, accelerating 4-NHE clearance and thereby attenuating PAH.

2. Materials and methods

2.1. Animal models

All animal care and experimental procedures were approved and conducted in accordance with the Institutional Animal Care and Use Committee of Jinzhou Medical University and conformed to the Guide for the Care and Use of Laboratory Animal published by the US National Institutes of Health. Male Sprague–Dawley rats (n=48; weighing 220–250 g) were purchased from Vital River Laboratories Animal Company (Beijing, China). The animals were intraperitoneally (i.p.) injected with a single dose of monocrotaline (MCT; 60 mg/kg; Sigma-Aldrich, St. Louis, MO) to induce severe PAH within 2 or 4 weeks (n=8 each group). For experiments involving pre-treatment with Alda-1 (Sigma-Aldrich Co., St. Louis, MO), MCT-injected rats were randomly divided into 3 groups, including the MCT group (n=12), the vehicle-alone group (n=6) administered 50% polyethylene glycol (PEG) and 50% dimethyl sulfoxide (DMSO) by volume, and the Alda-1 group (n=6). Control rats (n=8) were injected with an equal volume of 0.9% phosphate-buffered saline (PBS). The MCT-treated rats were subcutaneously implanted with mini-osmotic pumps (model 2004; ALZET, Cupertino, CA) and continuously infused with Alda-1 (10 mg kg⁻¹ d⁻¹) for 4 weeks.

2.2. 4-HNE-His adduct and malondialdehyde (MDA) assays

4-HNE and MDA levels were determined using the OxiSelect™ HNE-His Adduct ELISA Kit (Cell Biolabs, San Diego, CA) and the Lipid Peroxidation (MDA) Assay Kit (MAK085; Sigma-Aldrich), respectively. The enzyme-linked immunosorbent assay (ELISA) was performed according to the manufacturer's instructions, and the activity was measured using a Varioskan Flash microplate reader (Thermo Scientific, Waltham, MA).

2.3. ALDH2 activity assay

ALDH2 activity was measured using a ALDH2 Activity Assay Kit (GMS50131; GenMed, Pfizer, CA), according to the manufacturer's instructions. Enzyme activities were measured using a microplate reader by monitoring the production of NADPH at 340 nm.

2.4. Cell culture

Human pulmonary artery smooth muscle cells (HPASMCs) were purchased from ScienCell Research Laboratories (San Diego, CA) and were cultured in smooth muscle cell-growth medium (SMCM) at 37 °C, in a humidified atmosphere containing 5% CO₂. HPASMCs were used within 3–5 passages of the primary culture.

2.5. Cell-proliferation assay

Cell proliferation was quantified using the methyl thiazolyl tetrazolium (MTT) assay (Sigma-Aldrich). Briefly, cells were initially grown in 96-well microplates in complete SMCM for 24 h and, after washing with PBS, were incubated in serum-free SMCM medium for 24 h. The cells were then treated with different concentrations of 4-HNE for 24, 48, or 72 h. Absorbance of the cultures was measured at 570 nm using

a microplate reader.

2.6. BrdU-incorporation assay and cell cycle analysis

BrdU-incorporation assays were performed to measure HPASMC proliferation, using BrdU Flow kits (BD Pharmingen, Franklin Lakes, New Jersey). Briefly, HPASMCs were plated in 35 mm plates at a density of 1×10⁶ cells/well and were synchronized over 24 h under serum starvation. HPASMCs were then incubated with PBS or 0.1 μM 4-HNE for 48 h. When required, 20 μM Alda-1 was added 30 min before the addition of 4-HNE. The cells were labeled with BrdU, according to the manufacturer's instructions. The results were acquired using a BD LSRFortessa Cell Analyzer (Becton Dickinson, Franklin Lakes, New Jersey).

2.7. Analysis of cell migration and invasion

HPASMC migration was evaluated in scratch-induced, wound-healing assays [21]. HPASMCs were seeded into 6-well plates. Near-confluent HPASMCs were wounded by scraping with a standard 1-mL pipette tip to create a gap along the diameter of the well. HPASMC invasion was assessed by performing a Boyden chamber assay [22]. HPASMCs were seeded into the upper surface of an 8-μm pore size chamber, with serum-free SMCM medium, with or without 0.1 μM 4-HNE in the lower chamber. When required, 20 μM Alda-1 was added 30 min before the addition of 4-HNE.

2.8. Immunohistofluorescence

For double immunofluorescence staining, 5 μm-thick lung sections were incubated at 4 °C overnight with a mixture of mouse anti-4-HNE or anti-ALDH2 monoclonal antibodies (1: 200 dilution; Abcam, Cambridge, UK), and an anti-α-smooth muscle actin (α-SMA) mouse antibody (1:200 dilution; Abcam); alternatively, the primary antibody was substituted with an isotype control (1:200 dilution; Abcam). Immunohistofluorescence images were obtained using confocal microscopy (TCS-SP5, Leica Microsystems, Wetzlar, Germany).

2.9. Western blot analysis

Lung tissues (20 mg) or cells (1×10⁶) were sonicated in 100 μL radioimmunoprecipitation assay buffer (Aidlab, Beijing, China) and homogenized. HPASMC nuclear proteins were extracted using a Nuclear Protein Extraction Kit (Beyotime, Jiangsu, China), according to the manufacturer's instructions. Protein samples were separated by 10% sodium dodecyl sulfate-polyacrylamide gel electrophoresis and transferred to nitrocellulose membranes (Millipore, Billerica, MA). The membranes were then incubated overnight with the indicated primary antibodies at 4 °C. The following primary antibodies were used for western blotting: monoclonal antibodies against rabbit anti-cyclin D1, anti-c-Myc, anti-matrix metalloprotein (MMP)-9 and anti-MMP-2 (1:1000 dilution; Cell Signaling Technology, USA); polyclonal antibodies against rabbit anti-nuclear factor-kappa B (NF-κB) p65, anti-phospho-NF-κB p65, anti-nuclear factor of kappa light polypeptide gene enhancer in B-cells inhibitor, alpha (IκBα), and anti-phospho-IκBα (1:1000 dilution; Cell Signaling Technology, USA); monoclonal antibodies against mouse anti-4-HNE monoclonal antibody and mouse anti-ALDH2 (1: 500 dilution; Abcam, Cambridge, UK). Protein levels were analyzed using the Odyssey Infrared Imaging System (Li-Cor Biosciences, Lincoln, NE).

2.10. Real-time polymerase chain reaction (PCR)

Total RNA was extracted from HPASMCs using the RNeasy Pure Kit (Qiagen Biotech, Beijing, China), according to the manufacturer's instructions. The first-strand cDNA was reverse-transcribed from the

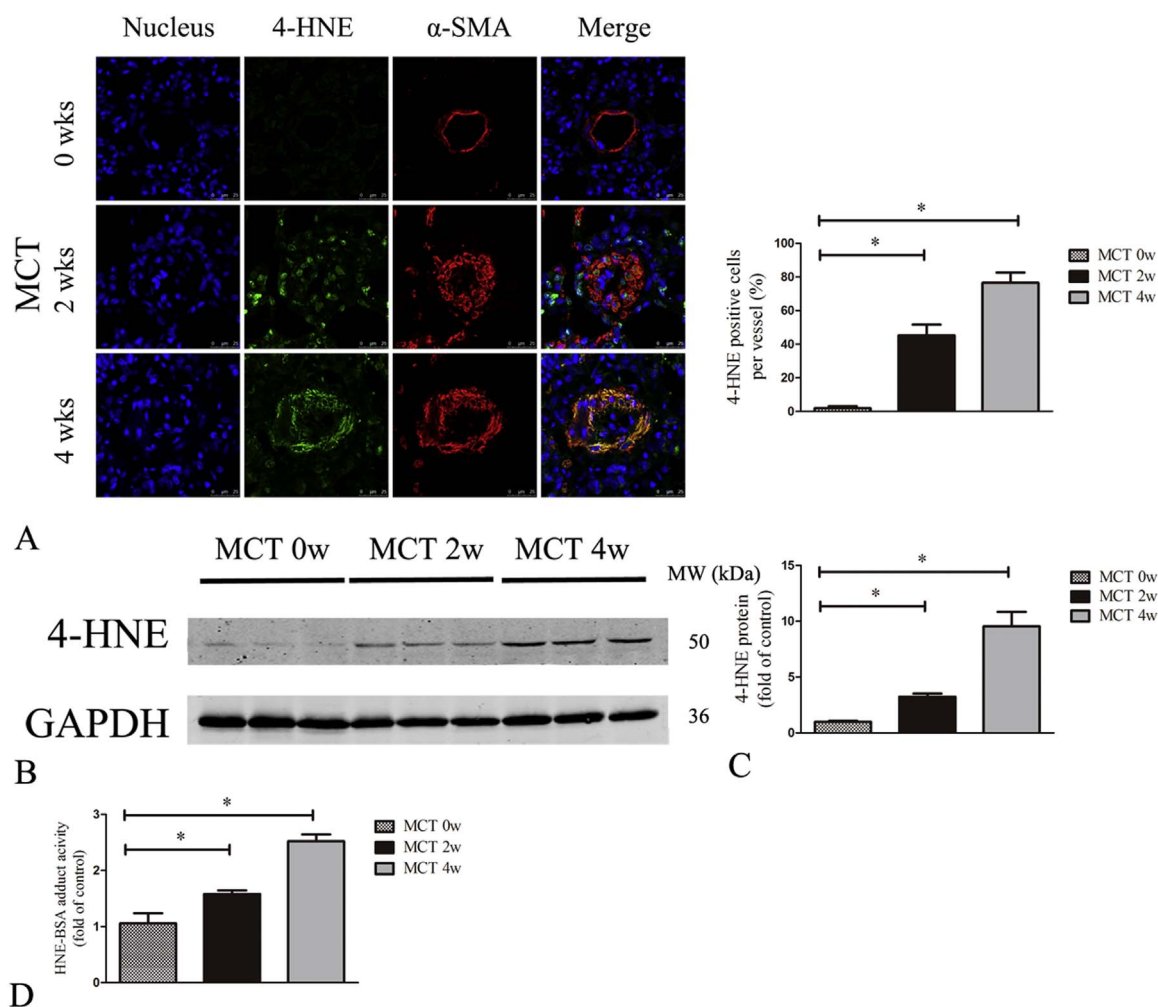


Fig. 1. MCT induced 4-HNE accumulation in rat lung tissues. (A) 4-HNE was detected in pulmonary arterial smooth muscle cells (PASMCs) in the lungs of rats with MCT-induced PAH. Representative immunofluorescence images of lung sections stained with anti-4-HNE antibodies (green) and anti- α -SMA antibodies (red), at 0, 2, and 4 weeks post-MCT stimulation. Cell nuclei were stained with 4',6-diamidino-2-phenylindole (DAPI) (blue). Compared with 0 week rats, 4-HNE levels in the pulmonary arterial media increased in rats with MCT-induced PAH, in terms of the percent nuclear localization. (B) 4-HNE expression in the lung tissue lysates, as determined by western blotting. (C) Quantification of protein levels from (B), relative to the control. * $P < 0.05$ ($n=3$). (D) 4-HNE levels in tissue lysates measured by ELISA. Data are presented as the mean \pm SD ($n=6$ in each group). * $P < 0.05$. (For interpretation of the references to color in this figure legend, the reader is referred to the web version of this article.)

total RNA using the Superscript III First-Strand Synthesis System (Invitrogen, Carlsbad, CA). Real-time PCR was performed with an Mx3000 P Real-Time PCR Detection System (Agilent, Santa Clara, CA). Data were analyzed using the $2^{-\Delta\Delta CT}$ method with GAPDH serving as an internal control [23]. The sequences of the forward and reverse primers used are shown in Table S1.

2.11. Cell transfection with small interfering RNA (siRNA) and ALDH2 lentiviral vector

HPASMCs were cultured from an initial density of 1×10^5 cells/mL to a monolayer and seeded into 6-well plates on the day before the transfection. After growing the cells to 50% confluency (24 h), they were transfected with siRNA targeting human *RelA* (NF- κ B p65 siRNA) or a scrambled siRNA (Scr-siRNA) (Santa Cruz Biotechnology, Santa Cruz, CA) at a final concentration of 30 nM in the culture supernatant. The sequences of the siRNAs were 5'-GAUGAGAUCUCCUA CUGUdTdT-3' for *RelA* and 5'-UUCUCCGAACGUGU CACGU TTdTdT-3' for Scr-siRNA. The siRNAs were transfected into HPASMCs using Lipofectamine (Invitrogen), following the manufacturer's recommended protocol [24].

A lentiviral vector (GENECHEM, Shanghai, China) was used to establish a stably transfected HPASMC cell line expressing ALDH2.

The retroviral packaging process was performed according to the manufacturer's protocol. Briefly, HPASMCs were seeded at 2×10^5 cells/well in 6-well plates 24 h prior to transfection. The HPASMCs were grown to approximately 50% confluence and transfected with the recombinant Lenti-OE vector ALDH2 in enhanced infection solution overnight. Subsequently, the virus-containing medium was replaced with 4 mL of fresh culture medium. Measurements were conducted 3 days after transfection by western blot and real-time PCR.

2.12. Hemodynamic measurements and evaluation of right ventricular hypertrophy

Sprague–Dawley rats were anesthetized with 1% pentobarbital sodium (40 mg/kg, i.p.). As an indicator of the mean pulmonary arterial pressure, right ventricular systolic pressure (RVSP) was measured using a guide-wire inserted into the right ventricle via the right jugular vein [25].

2.13. Analysis of pulmonary arterial morphology

Following the hemodynamic measurements, rats were sacrificed by cervical dislocation, and the lungs and hearts were harvested. Right

lung specimens were fixed in 4% paraformaldehyde (pH 7.4) for 24 h and then embedded in paraffin wax. Serial Section (5- μ m thickness) were stained with hematoxylin and eosin (H & E). Percent medial wall thickness (% MT), an estimate of the pulmonary arteriolar remodeling, was calculated as follows: wall thickness (%) = $[(\text{medial thickness} \times 2) / \text{external diameter}] \times 100\%$ [26].

2.14. Statistical analysis

Data are presented as the mean \pm SD and were analyzed using Prism 5 (GraphPad Software, La Jolla, CA). Group comparisons were performed using 1-way ANOVA, followed by a Newman–Keuls test. Differences were considered statistically significant at $P < 0.05$.

3. Results

3.1. Levels of 4-HNE in MCT-induced pulmonary rat arteries

Moderate proliferation of tunica media smooth muscle cells in pulmonary arteries was observed 2 weeks after MCT induction, which became more pronounced 4 weeks after induction. Double immunofluorescence staining revealed low levels of 4-HNE in the smooth muscle cells of the pulmonary vascular walls of control animals, and high 4-HNE levels in the pulmonary vascular walls of MCT-induced animals (Fig. 1A and B). Our data suggested that MCT injection led to a significant increase in 4-HNE levels in rat lung tissues (Fig. 1C and D). MCT-induced accumulation of 4-HNE in rat lung tissues was also detected at 2 and 4 weeks post-induction by ELISA (Fig. 1E).

3.2. The effect of 4-HNE on HPASMC proliferation

Pulmonary vascular remodeling induced by the proliferation and migration of smooth muscle cells is thought to be the main cause of PAH development [27]. To assess the role of 4-HNE in modulating HPASMC proliferation, the cells were administered different concentrations of 4-HNE (0.01–1 μ M). We observed that 4-HNE stimulated HPASMC proliferation in a dose-dependent manner, with a maximal effect elicited by a 0.1- μ M dose, at 48 h post-treatment (Fig. 2A). The results of BrdU-incorporation assays confirmed that 4-HNE treatment (0.1 and 1 μ M) significantly increased the proliferation of cultured HPASMCs ($P < 0.05$ vs. control; Fig. 2B). Western blot analysis showed that 4-HNE stimulated expression of the proliferative factors cyclin D1 and c-Myc in cultured HPASMCs in a dose-dependent manner (Fig. 2C–E). Similarly, 4-HNE increased cyclin D1 and *c-myc* mRNA levels in cultured HPASMCs (Fig. 2F and G). In parallel, 4-HNE treatment led to a reduction of cells in G0/G1 phase, while increasing the proportion of cells in S phase, relative to control HPASMCs (Fig. 2H).

3.3. Effect of 4-HNE on the migration of HPASMCs

The effect of 4-HNE on HPASMC migration *in vitro* was evaluated in scratch-wound and Boyden-chamber assays. 4-HNE treatment robustly enhanced HPASMC migration, increasing the migration area (Fig. 3A and B) and the number of migrated cells (Fig. 3C and D). MMP activation plays a key role in pulmonary vascular remodeling, resulting in the degradation of various components of the extracellular matrix (ECM) and mediating ECM remodeling, thereby inducing HPASMC migration [28]. 4-HNE induced MMP-9 and MMP-2 expression in cultured HPASMCs (Fig. 3E–G). Similarly, *MMP-9* and *MMP-2* mRNA levels in cultured HPASMCs were higher after 4-HNE treatment than those in control cells (Fig. 3H and I).

3.4. NF- κ B activation contributes to the effects of 4-HNE on cultured HPASMCs

Recently, the NF- κ B signaling pathway was found to play a role in oxidative stress in human and experimental PAH [29,30]. Incubation of HPASMCs with 4-HNE promoted phosphorylation and degradation of the NF- κ B inhibitor I κ B α , as well as phosphorylated NF- κ B p65 in the cytoplasm (Fig. 4A–C). In addition, 4-HNE treatment elicited an increase in nuclear NF- κ B p65 levels (Fig. 4D and E). Activation of the NF- κ B signaling pathway is a key mediator of MMP expression [34]. Knockdown of NF- κ B p65 levels with siRNA suppressed NF- κ B p65 expression, as determined by western blotting and real-time PCR (Fig. S1), and suppressed 4-HNE-induced MMP-9 and MMP-2 expression in cultured HPASMCs (Fig. 4F–H). Importantly, HPASMC migration in response to 4-HNE was blocked by NF- κ B p65 siRNA (Fig. 4I and J).

3.5. Activation of ALDH2 inhibits the effects of 4-HNE on cultured HPASMCs

ALDH2 expression was significantly reduced in HPASMCs stimulated with 4-HNE, as demonstrated by western blotting and real-time PCR analyses (Fig. 5A–D). We used a retrovirus-based vector to generate ALDH2-overexpressing HPASMCs. Compared with cells transduced with the empty vector, ALDH2 protein and mRNA levels were remarkably elevated in ALDH2-overexpressing HPASMCs (Fig. S2). Overexpression of ALDH2 in HPASMCs counteracted 4-HNE-induced cyclin D1 and c-Myc expression; similarly, treatment with the ALDH2 agonist Alda-1 (20 μ M) reduced 4-HNE-induced cyclin D1 and c-Myc expression (Fig. 5E–G). Importantly, ALDH2 overexpression and Alda-1 treatment prevented both 4-HNE-induced HPASMC proliferation and changes in the G0/G1- and S-phase populations (Fig. 5H and I). In addition, ALDH2 overexpression and Alda-1 treatment both inhibited 4-HNE-induced nuclear translocation of NF- κ B p65 (Fig. 5J–L). Boyden-chamber assay results revealed that 4-HNE-induced HPASMC migration was almost abolished by ALDH2 overexpression and by Alda-1 treatment (Fig. 5M and N).

3.6. Alda-1 activates ALDH2 to reduce MCT-induced pulmonary vascular remodeling and PAH

ALDH2 activity was significantly decreased *in vivo*. Furthermore, 4-HNE accumulation was significantly higher in MCT- and MCT+ vehicle-treated groups when compared with control group, and Alda-1 pretreatment significantly induced ALDH2 activity in the lungs of MCT-stimulated rats (Fig. 6A–C). In addition, the lung MDA levels significantly increased in the MCT- and MCT+ vehicle-treated groups compared with the control animals (32.38 ± 3.02 and 30.25 ± 2.12 nmol/mg protein, respectively, vs. 22.63 ± 2.72 nmol/mg protein in control rats, $P < 0.05$; Fig. 6D). However, Alda-1 pretreatment significantly reduced MCT-induced lung MDA contents (24.62 ± 1.92 nmol/mg protein; $P < 0.05$ vs. MCT or MCT+vehicle), as shown in Fig. 6D. RVSP and right ventricular hypertrophy index (RVHI) were significantly lower ($P < 0.05$) in the MCT+Alda-1 group (39.79 ± 4.17 and 0.34 ± 0.12 mm Hg, respectively) than in the MCT group (74.29 ± 5.21 and 0.68 ± 0.17 mm Hg, respectively) and MCT+vehicle group (68.92 ± 7.32 and 0.59 ± 0.14 mm Hg, respectively), as shown in Fig. 6E and F. However, the systemic pressure did not change significantly with Alda-1 treatment (Table S2). H & E staining revealed that the % MT was significantly lower in the MCT+Alda-1 group ($29.35 \pm 3.78\%$) than in the MCT and MCT + vehicle groups ($59.68 \pm 6.82\%$ and $60.39 \pm 5.91\%$, respectively; $P < 0.05$; Fig. 6G and H). Furthermore, Alda-1 pretreatment significantly reduced I κ B α phosphorylation and blocked the nuclear translocation of NF- κ B p65 in MCT-induced rat lung tissues (Fig. 6I–K).

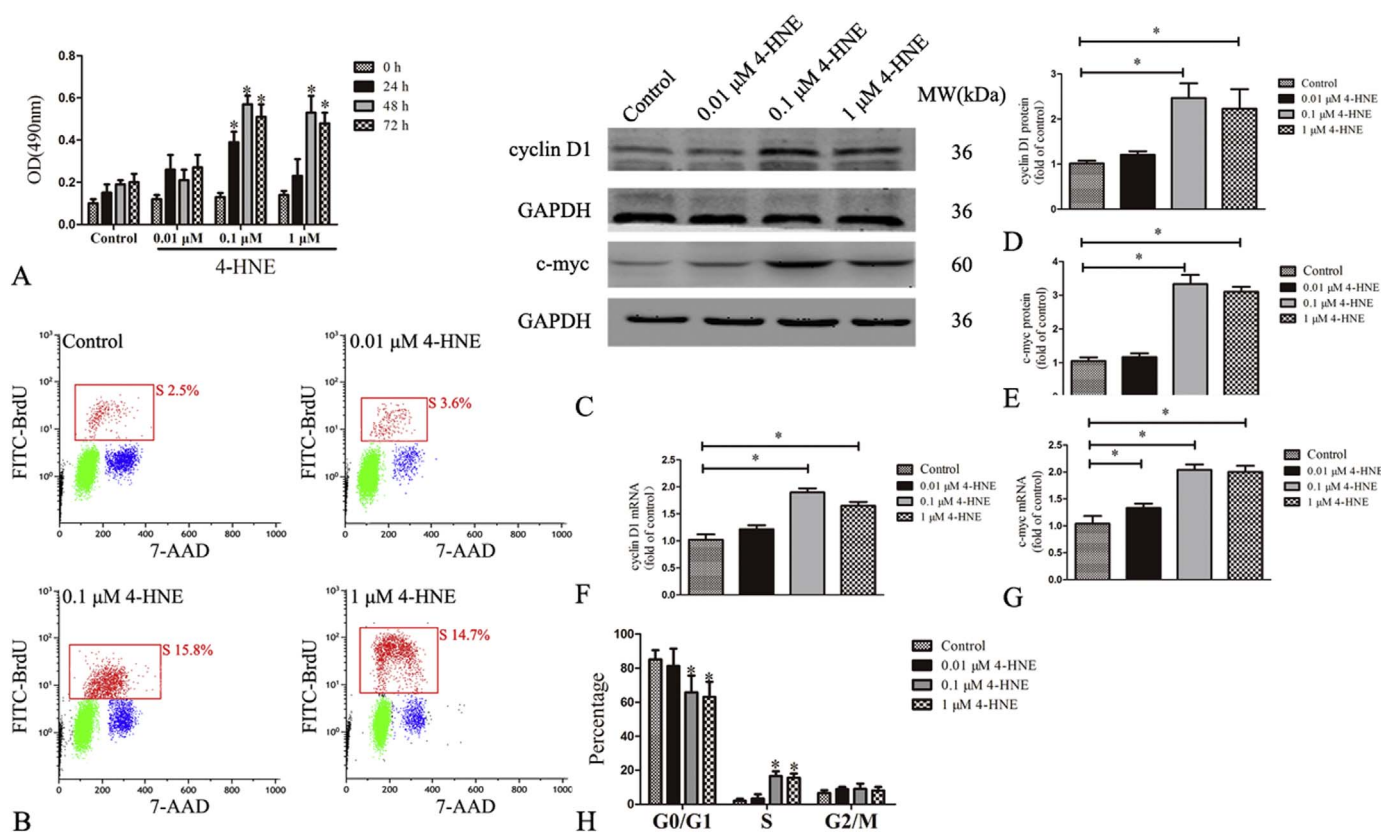


Fig. 2. The effect of 4-HNE on HPASMC proliferation *in vitro*. (A) The effect of different concentrations of 4-HNE (0.01, 0.1, and 1 μ M) on HPASMC proliferation, as determined by performing MTT assays. Cells were treated for 0, 24, 48, or 72 h. (B) The effect of a 48-h 4-HNE treatment (0.01, 0.1, and 1 μ M) on HPASMC DNA synthesis, as determined in BrdU assays. (C) HPASMC cyclin D1 and c-Myc expression, evaluated by western blotting. Cyclin D1 (D) and c-Myc (E) protein levels were quantified relative to the indicated control. * $P < 0.05$ ($n=3$). (F) HPASMC cyclin D1 and (G) *c-myc* mRNA levels, determined by real-time PCR. * $P < 0.05$ ($n=3$). (H) The effect of a 48-h 4-HNE treatment (0.01, 0.1, and 1 μ mol/L) on HPASMC proliferation, evaluated by assessing the distribution of cells in various phases of the cell cycle by flow cytometry. * $P < 0.05$ vs. control. Data are presented as the mean \pm SD ($n=6$ in each group).

4. Discussion

Although PAH treatment has continuously improved in recent years, the basic mechanism underlying PAH remains unclear [31]. Many therapeutic drugs continue to be designed and developed for clinical use, but they target a variety of classical signaling pathways, such as prostacyclin, endothelin, and nitric oxide pathways, which are often only effective in a subset of PAH patients [32–34]. Increasing evidence from both experimental animal models and patients has implicated oxidative stress in PAH pathogenesis [35,36].

MCT induces severe PAH and this animal model imitates certain key characteristics of human PAH, including pulmonary vascular remodeling, PASC proliferation, and oxidative stress [37,38]. In this study, our data revealed that 4-HNE levels were significantly elevated in the lungs of rats with MCT-induced PAH and that 4-HNE promoted the proliferation and migration of HPASMCs *in vitro*. Furthermore, Alda-1 pretreatment stimulated ALDH2 activity, which in turn attenuated MCT-induced 4-HNE levels and nuclear NF- κ B p65 translocation. This, in turn, was accompanied by reduced PAH and improved pulmonary vascular remodeling.

Abnormal PASC proliferation and migration are 2 critical pathological features of pulmonary vascular remodeling that act as driving forces in the initiation and development of PAH [39]. Reactive oxygen species play central roles in abnormal PASC proliferation [40,41]. In this study, we observed that low 4-HNE concentrations stimulated HPASMC proliferation *in vitro*, which was confirmed by the increased ratio of BrdU-positive total cells and the increased population of cells in the S phase of the cell cycle. Further, 4-HNE induced both mRNA and protein expression levels of the proliferation markers cyclin D1

and c-Myc in HPASMCs *in vitro* (Fig. 2). Data from previous studies also showed that 4-HNE induced human aortic smooth muscle cell proliferation and differentiation, and rat aortic smooth muscle cell proliferation, in a dose-dependent manner [42]. However, high concentrations of HNE initiated apoptosis by inducing endoplasmic reticulum stress and mitochondrial dysfunction in human colon carcinoma cells and neuroblastoma cells [43,44]. These findings indicated that the function of HNE is complex; whether it promotes proliferation, differentiation or cell apoptosis depends upon its concentration and the cell type involved.

MMPs are zinc-dependent proteases that play important roles in ECM degradation in many tissues, and participate in cell migration during normal development or vascular remodeling [45,46]. MMPs can be subdivided into multiple groups, such as collagenases, gelatinases (MMP-2 and MMP-9), stromelysins, and matrilysins, among others [47]. Moreover, the results of many studies have indicated that MMP-2 and MMP-9 expression is significantly higher in pulmonary arteries and PASCs of PAH patients than in control subjects [48,49]. Here, we showed that 4-HNE exposure induced HPASMC migration, and the expression of MMP-9 and MMP-2 significantly increased following 4-HNE stimulation *in vitro* (Fig. 3). 4-HNE also enhanced MMP-2 expression in vascular smooth muscle cells by activating the NF- κ B signaling pathway [10]. These results suggest that 4-HNE positively regulates HPASMC migration by increasing MMP-9 and MMP-2 expression.

NF- κ B is considered a crucial redox-sensitive transcription factor that consists of the p50, p52, c-Rel, RelB, and p65 proteins [50]. Under most non-stimulatory conditions, the NF- κ B p65 protein is localized to the cytoplasm, where it is bound by its inhibitor, I κ B α . Upon oxidative

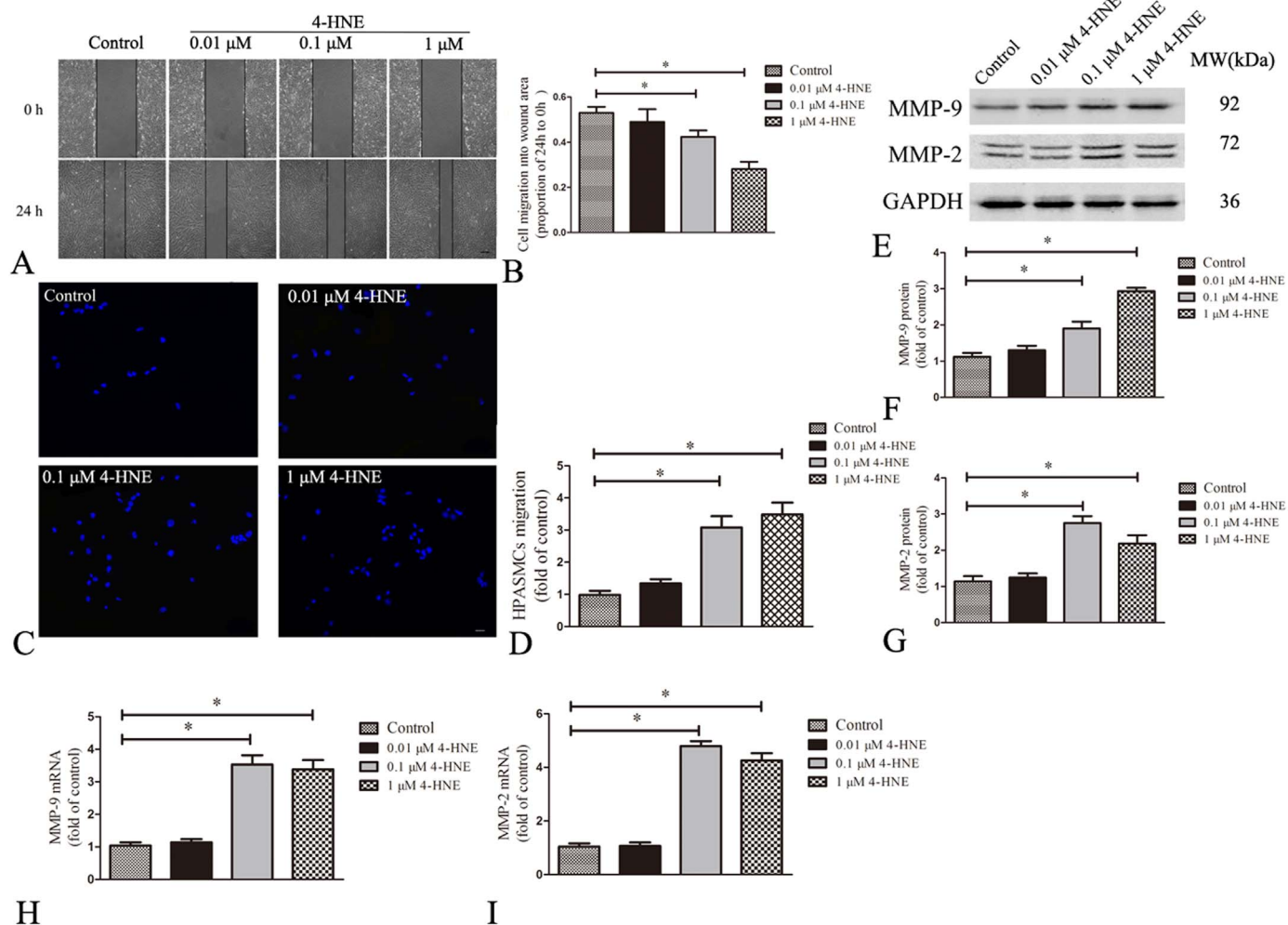


Fig. 3. Effect of 4-HNE on HPASMC migration *in vitro*. (A) Representative photographs showing invading cells after a 24-h treatment with different 4-HNE concentrations (0.01, 0.1, and 1 μM). Wounds were induced by scraping confluent cell layers with a 1-mL pipet tip. Confluent HPASMC monolayers were starved for 24 h in serum-free SMCM and incubated with 4-HNE for 24 h, when the migrated areas were counted. (B) Bar graph showing the migrated wound area of HPASMCs in response to 4-HNE. * $P < 0.05$ ($n=6$). (C) Migration of HPASMCs in response to a 24-h 4-HNE treatment, as determined in Boyden chamber assays. (D) Bar graph showing the number of migrated HPASMCs from (C). * $P < 0.05$ ($n=6$). (E) Western blot analysis of MMP-9 and MMP-2 protein levels in HPASMCs. (F) Statistical analysis of MMP-9 and (G) MMP-2 protein levels in HPASMCs. * $P < 0.05$ ($n=3$). (H) Levels of HPASMC *MMP-9* and (I) *MMP-2* mRNA, measured by real-time PCR. Data are presented as the mean \pm SD. * $P < 0.05$ ($n=3$ in each group).

stress injury, I κ B α is phosphorylated and degraded, resulting in the release of NF- κ B p65 dimers from the inhibitory complex and the translocation of NF- κ B p65 to the nucleus, where it stimulates the transcription of related genes [51]. We previously demonstrated that NF- κ B contributes to pulmonary vascular remodeling in an MCT-induced PAH rat model [52]. Further, lipid peroxidation products induce the proliferation and migration of HPASMCs by promoting NF- κ B activation [53]. In this study, we demonstrated that 4-HNE stimulated I κ B α phosphorylation and degradation, and subsequently induced nuclear translocation of NF- κ B p65 in HPASMCs *in vitro*. Furthermore, we confirmed that the MMP-9 and MMP-2 expression increased following 4-HNE induction, most likely by modulating NF- κ B signaling, which led to HPASMC migration (Fig. 4). Previous studies have suggested that NF- κ B is also involved in MMP-2 expression in rat glomerular mesangial cells and contributes to cell migration via increased MMP-9 expression in vascular smooth muscle cells *in vitro* [54,55]. Collectively, these results suggest that NF- κ B may be a critical downstream mediator of the migratory response of HPASMCs to 4-HNE induction.

ALDH2 is widely expressed in the lungs and is a key metabolic enzyme involved in 4-HNE detoxification [56]. ROS can inhibit ALDH2 dehydrogenase activity [57]. Data from recent studies have implicated ALDH2 and its polymorphisms in cardiovascular diseases [58], includ-

ing coronary artery disease [59], ischemia-reperfusion injury [60], and diabetic cardiomyopathy [61]. Alda-1, the small molecule activator of ALDH2, reduces LPS-induced NF- κ B p65 phosphorylation and nuclear translocation in human umbilical vein endothelial cells [62]. In this study, we confirmed that 4-HNE-induced HPASMC proliferation was prevented by ALDH2 or Alda-1 overexpression, both of which inhibited cyclin D1 and c-Myc expression. We also observed that ALDH2 overexpression or Alda-1 treatment alleviated 4-HNE-induced HPASMC migration by suppressing the nuclear translocation of NF- κ B p65 (Fig. 5). ALDH2 also contributes to nitroglycerin-induced nitric oxide formation in vascular smooth muscle cells [63], but the effect of ALDH2 on the pulmonary vasculature remains unknown. Future studies are required to determine whether ALDH2 contributes to vascular remodeling associated with PAH through nitric oxide signaling pathways.

It would be also interesting to establish whether ALDH2 activation contributes to MCT-induced PAH and pulmonary vascular remodeling. We demonstrated that pretreatment with Alda-1 significantly induced ALDH2 activity in pulmonary tissues and reduced the levels of 4-HNE and MDA, ultimately improving MCT-induced PAH in the rat model. Previous studies have provided evidence that excessive 4-HNE inhibits ALDH2 activity [64,65]. We also observed that Alda-1 pretreatment significantly blocked MCT-induced NF- κ B p65 nuclear translocation in

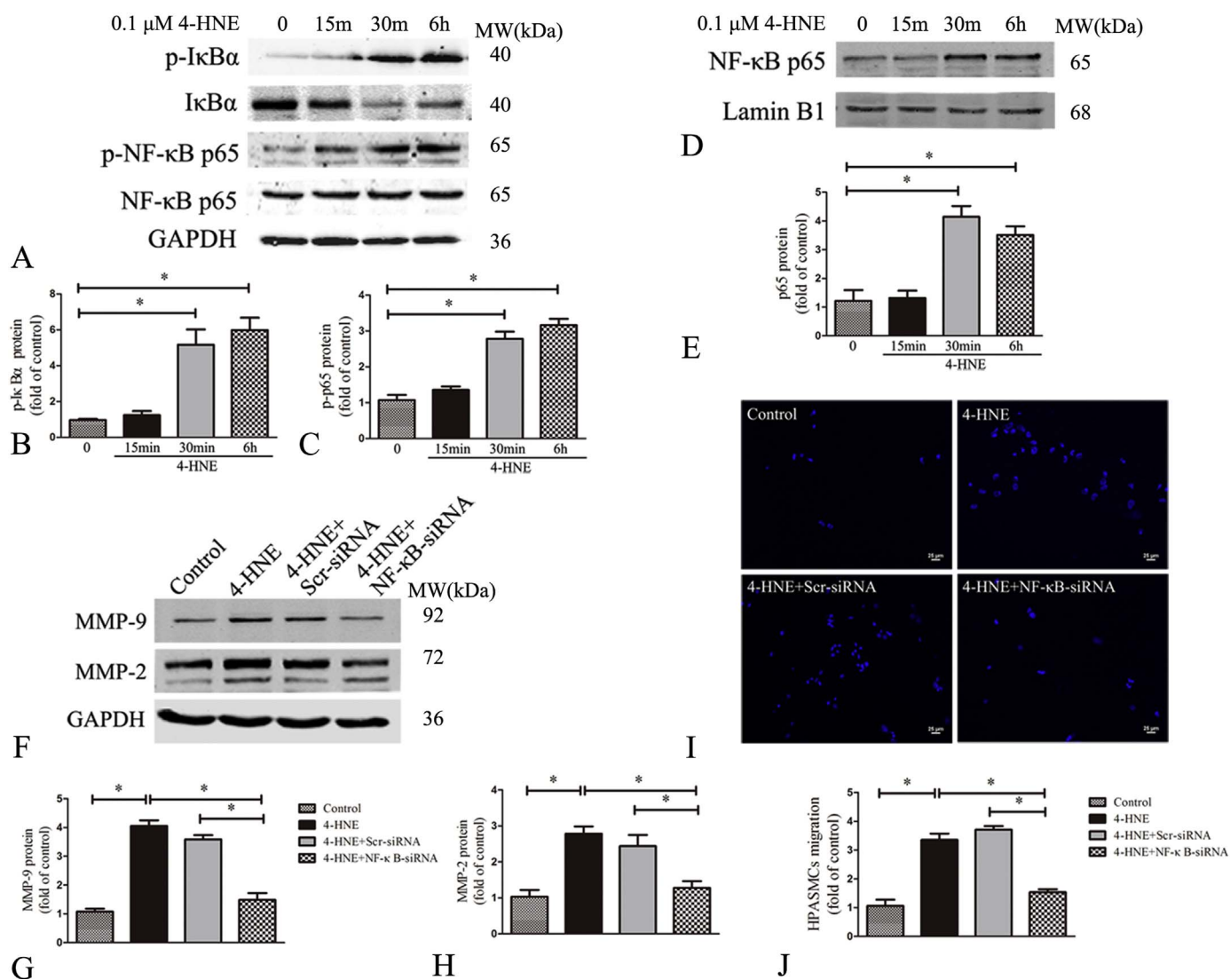


Fig. 4. The effect of 4-HNE on the nuclear translocation of NF-κB p65 in HPASMCs. Confluent HPASMC monolayers were starved for 24 h in serum-free SMCM and stimulated with 4-HNE (0.1 μM) for the indicated times. (A) Western blot analysis of phospho-IκBα, IκBα, phospho-NF-κB p65, NF-κB p65, and GAPDH protein levels in HPASMCs. (B) Statistical analysis of the phospho-IκBα/IκBα and (C) phospho-NF-κB p65/NF-κB p65 levels in HPASMCs. **P* < 0.05 (n=6). (D) Representative western blot showing NF-κB p65 in nuclear extracts from cultured HPASMCs treated for various times with 0.1 μM 4-HNE, with lamin B1 used as a loading control. (E) Statistical analysis of the NF-κB p65/lamin B1 levels. **P* < 0.05 (n=3). (F) Western blot showing the effect of siRNA knockdown of *RelA* (NF-κB p65 siRNA) on MMP-9 and MMP-2 expression in response to 0.1 μM 4-HNE. (G) Statistical analysis of MMP-9 and (H) MMP-2 expression in HPASMCs. **P* < 0.05 (n=3). (I) The effect of NF-κB p65 siRNA on the migration of HPASMCs in response to 0.1 μM 4-HNE treatment. (J) Bar graph showing the number of migrated HPASMCs from I. Data are presented as the mean ± SD. **P* < 0.05 (n=3 in each group).

pulmonary tissues (Fig. 6). These results suggested that ALDH2 may inhibit activation of the NF-κB signaling pathway induced by 4-HNE in HPASMCs, suggesting a key role for ALDH2 in preventing MCT-induced PAH.

5. Limitations

It should be noted that we only examined the role of ALDH2 in MCT-induced PAH in rats, without evaluating using other animal models of PAH, such as hypoxia-induced PAH or Sugen-5416/hypoxia-induced PAH. Another, MCT-induced PAH is only a pro-inflammatory and oxidative stress relevant animal model, whereas PAH in humans is considered to develop by multiple pathogenic factors. Although this MCT-induced PAH model might emphasize the potential effects of ALDH2, whether these characteristics influence human PAH is unknown. Therefore, further study is warranted to define the role of ALDH2 in PAH.

6. Conclusions

Our results indicated that 4-NHE accumulation plays an important role in the proliferation and migration of pulmonary smooth muscle cells. ALDH2 significantly attenuated 4-HNE-induced cell proliferation and migration, possibly by inhibiting activation of the NF-κB pathway. This mechanism may provide a novel therapeutic strategy for treating PAH.

Author contributions

Tao Xu and Aimei Wang conceived and designed the experiments. Tao Xu, Shuangyue Liu, Tingting Ma, Ziyi Jia, and Zhifei Zhang performed the experiments. Tingting Ma and Ziyi Jia analyzed the data. Zhifei Zhang and Aimei Wang contributed reagents/materials/analysis tools; Tao Xu and Shuangyue Liu wrote the draft, Tao Xu and Aimei Wang checked and revised. All authors approved to submit this version to this publication.

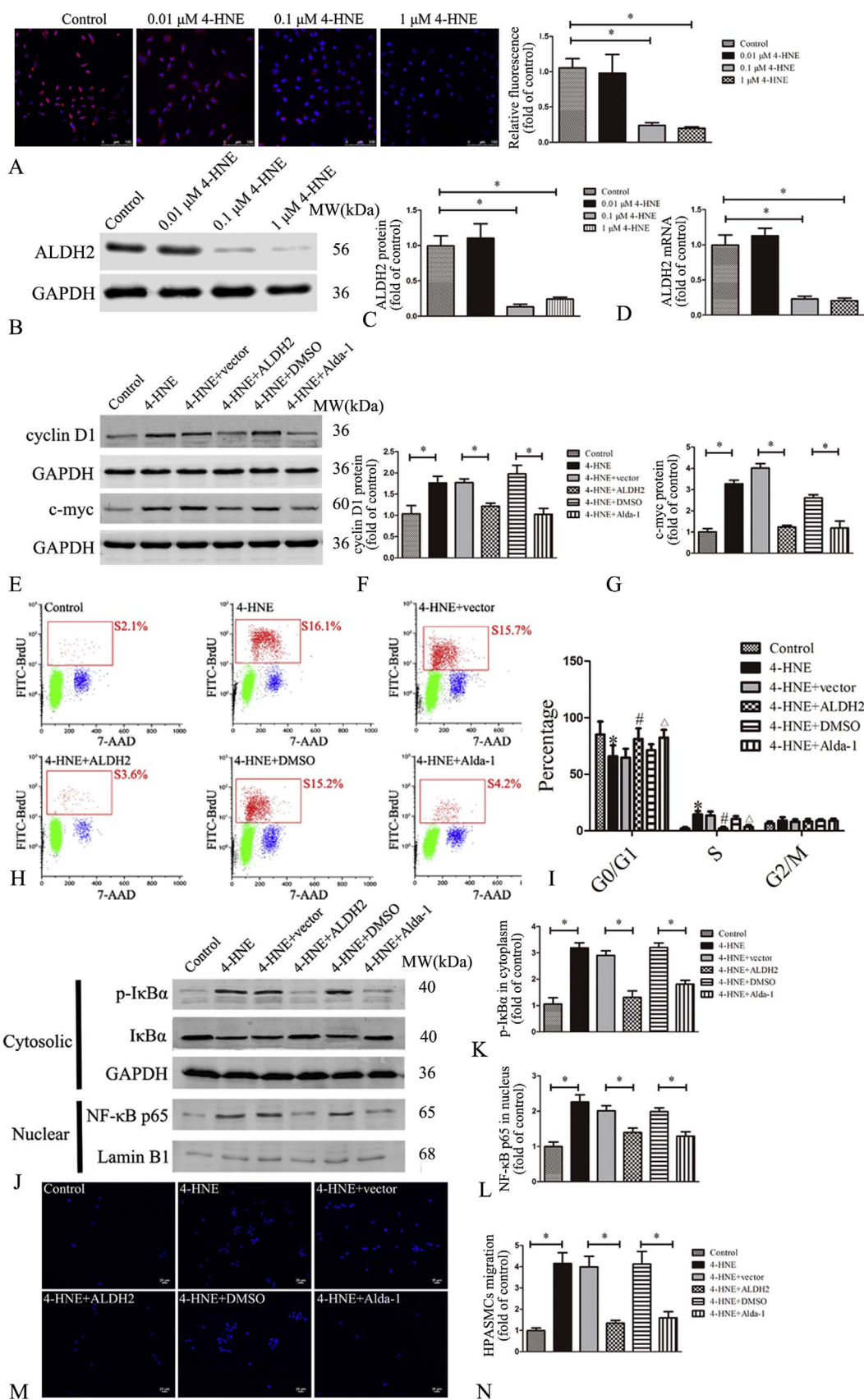


Fig. 5. The role of ALDH2 in HPASMC proliferation and migration, and its effect on the response of NF-κB signaling to 4-HNE *in vitro*. (A) ALDH2 is expressed in HPASMCs upon 4-HNE treatment. Representative immunofluorescence images showing ALDH2 (red) and cell nuclei (blue) in HPASMCs. (B) Western blot analysis of ALDH2 levels in HPASMCs. (C) Statistical analysis of ALDH2 expression in HPASMCs from (B). **P* < 0.05 (n=3). (D) Real-time PCR analysis of *ALDH2* mRNA levels in HPASMCs. **P* < 0.05 (n=3). (E) Western blot showing the effect of ALDH2 overexpression or Alda-1 (an ALDH2 agonist; 20 μM) on cyclin D1 and c-Myc HPASMC levels in response to 0.1 μM 4-HNE. (F) Statistical analysis of cyclin D1 and (G) c-Myc expression in HPASMCs. **P* < 0.05 (n=3). (H) The effect of ALDH2 overexpression or Alda-1 (20 μM) on HPASMC proliferation in response to a 48-h 4-HNE

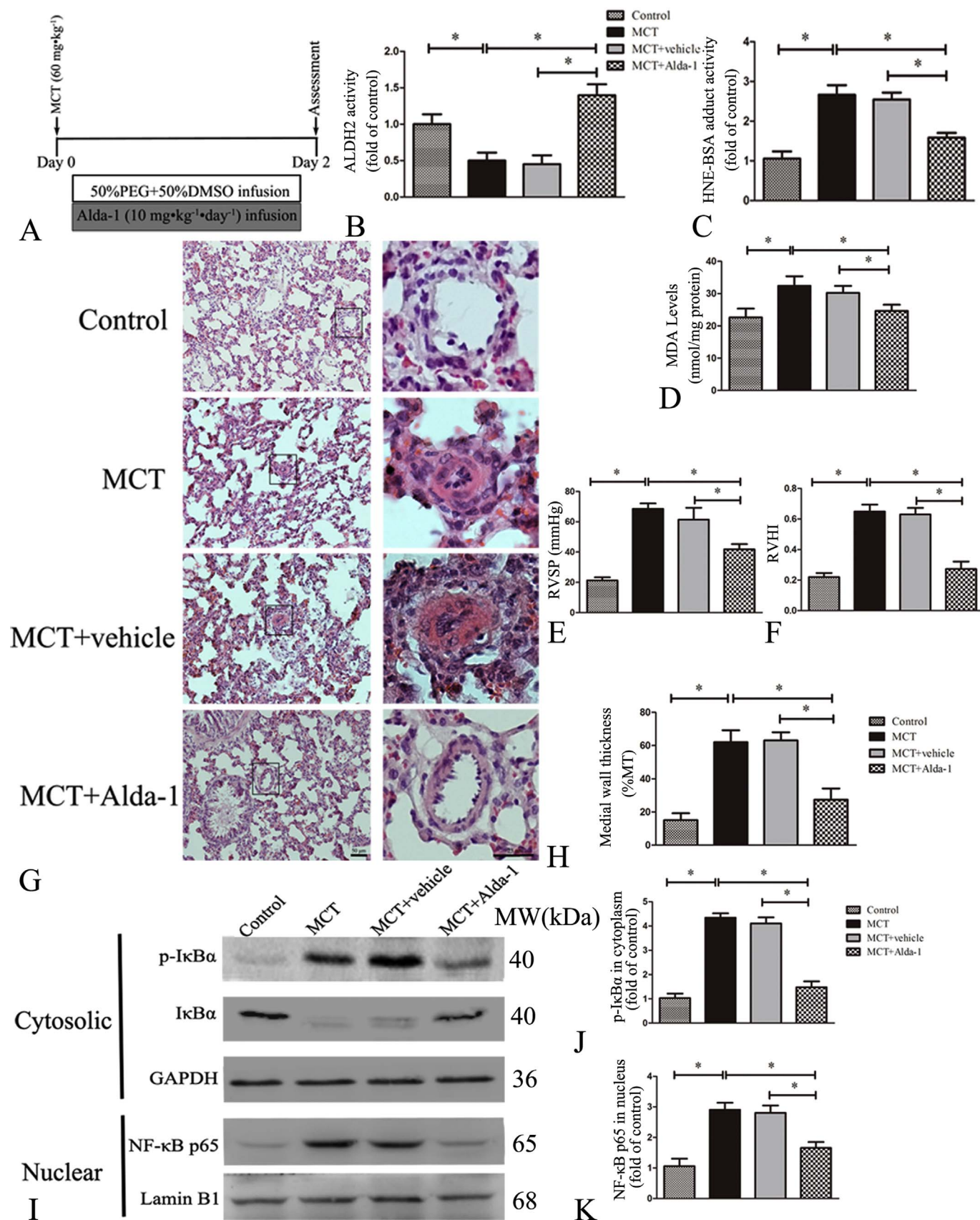


Fig. 6. Alda-1 prevents the development of PAH and pulmonary vascular remodeling *in vivo*. (A) Experimental protocol for examining the effect of Alda-1 treatment on MCT-induced PAH. (B) ALDH2 activity, and (C) 4-HNE and (D) MDA levels in the rat lung tissue, as measured by ELISA. Statistical analysis of (E) RVSP and (F) RVHI in PAH rats treated with Alda-1 (10 mg kg⁻¹ d⁻¹), at 4 weeks post-MCT challenge. **P* < 0.05 (n=6). (G) Representative images of H & E-stained pulmonary arteries from each group of animals. (H) Pulmonary artery medial wall thickness, measured in PAH rats treated with Alda-1, at 4 weeks post-MCT challenge. The medial wall thickness of the pulmonary arterioles (25–150 mm external diameter) was measured in H & E-stained lung sections. The medial wall thickness is expressed as specified in the Materials and Methods section (n=6). (I) The effect of ALDH2 on the nuclear translocation of NF-κB in the lungs. (J) Statistical analysis of cytoplasmic phospho-IκBα/IκBα levels and (K) nuclear NF-κB p65/lamin B1 levels. The data are presented as the mean ± SD. **P* < 0.05 (n=3).

Fundings

This work was supported by the National Natural Science Foundation of China [Grant Number 81674036], Liaoning Science and Technology Program [Grant Number 2014022029], Liaoning Education Program [Grant Number L2015316], Undergraduate of Liaoning Province Innovation and Entrepreneurship Training Program [Grant Number 201410160023].

Appendix A. Supporting material

Supplementary data associated with this article can be found in the online version at <http://dx.doi.org/10.1016/j.redox.2016.12.019>.

References

- [1] M. Humbert, D. Montani, O.V. Evgenov, G. Simonneau, Definition and classification of pulmonary hypertension, *Handb. Exp. Pharmacol.* 218 (2013) 3–29. http://dx.doi.org/10.1007/978-3-642-38664-0_1.
- [2] J. Takahashi, M. Orcholski, K. Yuan, V. de Jesus Perez, PDGF-dependent beta-catenin activation is associated with abnormal pulmonary artery smooth muscle cell proliferation in pulmonary arterial hypertension, *FEBS Lett.* 590 (1) (2016) 101–109. <http://dx.doi.org/10.1002/1873-3468.12038>.
- [3] Z. Kang, Y. Ji, G. Zhang, Y. Qu, L. Zhang, W. Jiang, Ponatinib attenuates experimental pulmonary arterial hypertension by modulating Wnt signaling and vasohibin-2/vasohibin-1, *Life Sci.* 148 (2016) 1–8. <http://dx.doi.org/10.1016/j.lfs.2016.02.017>.
- [4] J.P. Fessel, J.D. West, Redox biology in pulmonary arterial hypertension (2013 Grover Conference Series), *Pulm. Circ.* 5 (4) (2015) 599–609. <http://dx.doi.org/10.1086/683814>.
- [5] G.S. Reis, V.S. Augusto, A.P. Silveira, A.A. Jordao Jr., J. Baddini-Martinez, O. Poli Neto, A.J. Rodrigues, P.R. Evora, Oxidative-stress biomarkers in patients with pulmonary hypertension, *Pulm. Circ.* 3 (4) (2013) 856–861. <http://dx.doi.org/10.1086/674764>.
- [6] M. Csala, T. Kardon, B. Legeza, B. Lizak, J. Mandl, E. Margittai, F. Puskas, P. Szaraz, P. Szelenyi, G. Banhegyi, On the role of 4-hydroxynonenal in health and disease, *Biochim. Biophys. Acta* 1852 (5) (2015) 826–838. <http://dx.doi.org/10.1016/j.bbadis.2015.01.015>.
- [7] H. Zhong, H. Yin, Role of lipid peroxidation derived 4-hydroxynonenal (4-HNE) in cancer: focusing on mitochondria, *Redox Biol.* 4 (2015) 193–199. <http://dx.doi.org/10.1016/j.redox.2014.12.011>.
- [8] G. Leonarduzzi, E. Chiarpotto, F. Biasi, C. Des Rosiers, Circulating 4-hydroxynonenal and cholesterol oxidation products in atherosclerosis, *Mol. Nutr. Food Res.* 49 (11) (2005) 1044–1049. <http://dx.doi.org/10.1002/mnfr.200500090>.
- [9] C. Asselin, B. Bouchard, J.C. Tardif, C. Des Rosiers, Circulating 4-hydroxynonenal-protein thioether adducts assessed by gas chromatography-mass spectrometry are increased with disease progression and aging in spontaneously hypertensive rats, *Free Radic. Biol. Med.* 41 (1) (2006) 97–105. <http://dx.doi.org/10.1016/j.freeradbiomed.2006.03.011>.
- [10] S.J. Lee, K.W. Seo, M.R. Yun, S.S. Bae, W.S. Lee, K.W. Hong, C.D. Kim, 4-Hydroxynonenal enhances MMP-2 production in vascular smooth muscle cells via mitochondrial ROS-mediated activation of the Akt/NF-kappaB signaling pathways, *Free Radic. Biol. Med.* 45 (10) (2008) 1487–1492. <http://dx.doi.org/10.1016/j.freeradbiomed.2008.08.022>.
- [11] H. Kakishita, Y. Hattori, Vascular smooth muscle cell activation and growth by 4-hydroxynonenal, *Life Sci.* 69 (6) (2001) 689–697.
- [12] S.J. Chapple, X. Cheng, G.E. Mann, Effects of 4-hydroxynonenal on vascular endothelial and smooth muscle cell redox signaling and function in health and disease, *Redox Biol.* 1 (2013) 319–331. <http://dx.doi.org/10.1016/j.redox.2013.04.001>.
- [13] P.W. Buehler, J.H. Baek, C. Lisk, I. Connor, T. Sullivan, D. Kominsky, S. Majka, K.R. Stenmark, E. Nozik-Grayck, J. Bonaventura, D.C. Irwin, Free hemoglobin induction of pulmonary vascular disease: evidence for an inflammatory mechanism, *Am. J. Physiol. Lung Cell. Mol. Physiol.* 303 (4) (2012) L312–L326. <http://dx.doi.org/10.1152/ajplung.00074.2012>.
- [14] K. Semen, O. Yelisyeyeva, I. Jarocka-Karpowicz, D. Kaminsky, L. Solovey, E. Skrzydlewska, O. Yavorskiy, Sildenafil reduces signs of oxidative stress in pulmonary arterial hypertension: evaluation by fatty acid composition, level of hydroxynonenal and heart rate variability, *Redox Biol.* 7 (2016) 48–57. <http://dx.doi.org/10.1016/j.redox.2015.11.009>.
- [15] C.H. Chen, J.C. Ferreira, E.R. Gross, D. Mochly-Rosen, Targeting aldehyde dehydrogenase 2: new therapeutic opportunities, *Physiol. Rev.* 94 (1) (2014) 1–34. <http://dx.doi.org/10.1152/physrev.00017.2013>.
- [16] A. Daiber, M. Oelze, P. Wenzel, J.M. Wickramanayake, S. Schuhmacher, T. Jansen, K.J. Lackner, M. Torzewski, T. Munzel, Nitrate tolerance as a model of vascular dysfunction: roles for mitochondrial aldehyde dehydrogenase and mitochondrial oxidative stress, *Pharmacol. Rep.* 61 (1) (2009) 33–48.
- [17] C.H. Chen, L. Sun, D. Mochly-Rosen, Mitochondrial aldehyde dehydrogenase and cardiovascular diseases, *Cardiovasc. Res.* 88 (1) (2010) 51–57. <http://dx.doi.org/10.1093/cvr/cvq192>.
- [18] P.P. Hao, L. Xue, X.L. Wang, Y.G. Chen, J.L. Wang, W.Q. Ji, F. Xu, S.J. Wei, Y. Zhang, Association between aldehyde dehydrogenase 2 genetic polymorphism and serum lipids or lipoproteins: a meta-analysis of seven East Asian populations, *Atherosclerosis* 212 (1) (2010) 213–216. <http://dx.doi.org/10.1016/j.atherosclerosis.2010.05.024>.
- [19] Y. Zhao, C. Wang, Glu504Lys single nucleotide polymorphism of aldehyde dehydrogenase 2 gene and the risk of human diseases, *BioMed Res. Int.* 2015 (2015) 174050. <http://dx.doi.org/10.1155/2015/174050>.
- [20] X.X. Ma, S.Z. Zheng, Y. Shu, Y. Wang, X.P. Chen, Association between carotid, *Chin. Med. J.* 129 (12) (2016) 1413–1418. <http://dx.doi.org/10.4103/0366-6999.183413>.
- [21] L. Deng, F.J. Blanco, H. Stevens, R. Lu, A. Caudrillier, M. McBride, J.D. McClure, J. Grant, M. Thomas, M. Frid, K. Stenmark, K. White, A.G. Seto, N.W. Morrell, A.C. Bradshaw, M.R. MacLean, A.H. Baker, MicroRNA-143 activation regulates smooth muscle and endothelial cell crosstalk in pulmonary arterial hypertension, *Circ. Res.* 117 (10) (2015) 870–883. <http://dx.doi.org/10.1161/CIRCRESAHA.115.306806>.
- [22] E.A. Goncharova, D.A. Goncharov, V.P. Krymskaya, Assays for in vitro monitoring of human airway smooth muscle (ASM) and human pulmonary arterial vascular smooth muscle (VSM) cell migration, *Nature Protoc.* 1 (2006), 2006, pp. 2933–2939. <http://dx.doi.org/10.1038/nprot.2006.434>.
- [23] K.J. Livak, T.D. Schmittgen, Analysis of relative gene expression data using real-time quantitative PCR and the 2^{-Delta Delta C(T)} method, *Methods* 25 (4) (2001) 402–408. <http://dx.doi.org/10.1006/meth.2001.1262>.
- [24] M. Kadowaki, S. Mizuno, Y. Demura, S. Ameshima, I. Miyamori, T. Ishizaki, Effect of hypoxia and Beraprost sodium on human pulmonary arterial smooth muscle cell proliferation: the role of p27kip1, *Respir. Res.* 8 (2007) 77. <http://dx.doi.org/10.1186/1465-9921-8-77>.
- [25] R.J. van Suylen, J.F. Smits, M.J. Daemen, Pulmonary artery remodeling differs in hypoxia- and monocrotaline-induced pulmonary hypertension, *Am. J. Respir. Crit. Care Med.* 157 (5 Pt 1) (1998) 1423–1428. <http://dx.doi.org/10.1164/ajrccm.157.5.9709050>.
- [26] B.O. Okoye, P.D. Losty, D.A. Lloyd, J.R. Gosney, Effect of prenatal glucocorticoids on pulmonary vascular muscularization in nitrofen-induced congenital diaphragmatic hernia, *J. Pediatr. Surg.* 33 (1) (1998) 76–80.
- [27] R.J. Davies, N.W. Morrell, Molecular mechanisms of pulmonary arterial hypertension: role of mutations in the bone morphogenetic protein type II receptor, *Chest* 134 (6) (2008) 1271–1277. <http://dx.doi.org/10.1378/chest.08.1341>.
- [28] A. Vieillard-Baron, E. Frisdal, S. Eddahibi, I. Deprez, A.H. Baker, A.C. Newby, P. Berger, M. Levame, B. Raffestin, S. Adnot, M.P. d'Ortho, Inhibition of matrix metalloproteinases by lung TIMP-1 gene transfer or doxycycline aggravates pulmonary hypertension in rats, *Circ. Res.* 87 (5) (2000) 418–425.
- [29] Q. Wang, X.R. Zuo, Y.Y. Wang, W.P. Xie, H. Wang, M. Zhang, Monocrotaline-induced pulmonary arterial hypertension is attenuated by TNF-alpha antagonists via the suppression of TNF-alpha expression and NF-kappaB pathway in rats, *Vasc. Pharmacol.* 58 (1–2) (2013) 71–77. <http://dx.doi.org/10.1016/j.vph.2012.07.006>.
- [30] M. Wynants, L. Vengethasamy, A. Ronisz, B. Meyns, M. Delcroix, R. Quarck, NF-kappaB pathway is involved in CRP-induced effects on pulmonary arterial endothelial cells in chronic thromboembolic pulmonary hypertension, *Am. J. Physiol. Lung Cell. Mol. Physiol.* 305 (12) (2013) L934–L942. <http://dx.doi.org/10.1152/ajplung.00034.2013>.
- [31] M. Cojocaru, I.M. Cojocaru, I. Silosi, C.D. Vrabie, Associated pulmonary arterial hypertension in connective tissue diseases, *Maedica* 6 (2) (2011) 141–145.
- [32] I.M. Lang, S.P. Gaine, Recent advances in targeting the prostacyclin pathway in pulmonary arterial hypertension, *Eur. Respir. Rev.: Off. J. Eur. Respir. Soc.* 24 (138) (2015) 630–641. <http://dx.doi.org/10.1183/16000617.0067-2015>.
- [33] R. Madonna, N. Cocco, R. De Caterina, Pathways and drugs in pulmonary arterial hypertension - focus on the role of endothelin receptor antagonists, *Cardiovasc. Drugs Ther.* 29 (5) (2015) 469–479. <http://dx.doi.org/10.1007/s10557-015-6605-6>.
- [34] J.R. Klinger, S.H. Abman, M.T. Gladwin, Nitric oxide deficiency and endothelial dysfunction in pulmonary arterial hypertension, *Am. J. Respir. Crit. Care Med.* 188 (6) (2013) 639–646. <http://dx.doi.org/10.1164/rccm.201304-0686PP>.
- [35] P. Crosswhite, Z. Sun, Nitric oxide, oxidative stress and inflammation in pulmonary arterial hypertension, *J. Hypertens.* 28 (2) (2010) 201–212. <http://dx.doi.org/10.1097/HJH.0b013e328332bcd8>.
- [36] B. Van Houten, Pulmonary arterial hypertension is associated with oxidative, *Am. J. Respir. Crit. Care Med.* 192 (2) (2015) 129–130. <http://dx.doi.org/10.1164/rccm.201505-0904ED>.
- [37] N. Zhu, X. Zhao, Y. Xiang, S. Ye, J. Huang, W. Hu, L. Lv, C. Zeng, Thymoquinone attenuates monocrotaline-induced pulmonary artery hypertension via inhibiting pulmonary arterial remodeling in rats, *Int. J. Cardiol.* 221 (2016) 587–596. <http://dx.doi.org/10.1016/j.ijcard.2016.06.192>.
- [38] Y. Kishimoto, T. Kato, M. Ito, Y. Azuma, Y. Fukasawa, K. Ohno, S. Kojima, Hydrogen ameliorates pulmonary hypertension in rats by anti-inflammatory and antioxidant effects, *J. Thorac. Cardiovasc. Surg.* 150 (3) (2015). <http://dx.doi.org/10.1016/j.jtcvs.2015.05.052>.
- [39] M. Humbert, G. Monti, M. Fartoukh, A. Magnan, F. Brenot, B. Rain, F. Capron, P. Galanaud, P. Duroux, G. Simonneau, D. Emilie, Platelet-derived growth factor expression in primary pulmonary hypertension: comparison of HIV seropositive and HIV seronegative patients, *Eur. Respir. J.* 11 (3) (1998) 554–559.
- [40] K.Y. Hood, A.C. Montezano, A.P. Harvey, M. Nilsen, M.R. MacLean, R.M. Touyz, Nicotinamide adenine dinucleotide phosphate oxidase-mediated redox signaling and vascular remodeling by 16alpha-Hydroxysterone in human pulmonary artery cells: implications in pulmonary arterial hypertension, *Hypertension* 68 (3) (2016) 796–808. <http://dx.doi.org/10.1161/HYPERTENSIONAHA.116.07668>.
- [41] D. Guo, J. Gu, H. Jiang, A. Ahmed, Z. Zhang, Y. Gu, Inhibition of pyruvate kinase

- M2 by reactive oxygen species contributes to the development of pulmonary arterial hypertension, *J. Mol. Cell. Cardiol.* 91 (2016) 179–187. <http://dx.doi.org/10.1016/j.jmcc.2016.01.009>.
- [42] J. Ruef, G.N. Rao, F. Li, C. Bode, C. Patterson, A. Bhatnagar, M.S. Runge, Induction of rat aortic smooth muscle cell growth by the lipid peroxidation product 4-hydroxy-2-nonenal, *Circulation* 97 (11) (1998) 1071–1078.
- [43] B. Vizio, G. Poli, E. Chiarpotto, F. Biasi, 4-hydroxynonenal and TGF-beta1 concur in inducing antiproliferative effects on the CaCo-2 human colon adenocarcinoma cell line, *BioFactors* 24 (1–4) (2005) 237–246.
- [44] M. Dodson, Q. Liang, M.S. Johnson, M. Redmann, N. Fineberg, V.M. Darley-Usmar, J. Zhang, Inhibition of glycolysis attenuates 4-hydroxynonenal-dependent autophagy and exacerbates apoptosis in differentiated SH-SY5Y neuroblastoma cells, *Autophagy* 9 (12) (2013) 1996–2008.
- [45] X. Zhao, J. Kong, Y. Zhao, X. Wang, P. Bu, C. Zhang, Y. Zhang, Gene silencing of TACE enhances plaque stability and improves vascular remodeling in a rabbit model of atherosclerosis, *Sci. Rep.* 5 (2015) 17939. <http://dx.doi.org/10.1038/srep17939>.
- [46] E. Revuelta-Lopez, J. Castellano, S. Roura, C. Galvez-Monton, L. Nasarre, S. Benitez, A. Bayes-Genis, L. Badimon, V. Llorente-Cortes, Hypoxia induces metalloproteinase-9 activation and human vascular smooth muscle cell migration through low-density lipoprotein receptor-related protein 1-mediated Pyk2 phosphorylation, *Arterioscler., Thromb., Vasc. Biol.* 33 (12) (2013) 2877–2887. <http://dx.doi.org/10.1161/ATVBAHA.113.302323>.
- [47] A. Pardo, S. Cabrera, M. Maldonado, M. Selman, Role of matrix metalloproteinases in the pathogenesis of idiopathic pulmonary fibrosis, *Respir. Res.* 17 (2016) 23. <http://dx.doi.org/10.1186/s12931-016-0343-6>.
- [48] S.L. Tiede, M. Wassenberg, K. Christ, R.T. Schermuly, W. Seeger, F. Grimminger, H.A. Ghofrani, H. Gall, Biomarkers of tissue remodeling predict survival in patients with pulmonary hypertension, *Int. J. Cardiol.* 223 (2016) 821–826. <http://dx.doi.org/10.1016/j.ijcard.2016.08.240>.
- [49] X.M. Wang, K. Shi, J.J. Li, T.T. Chen, Y.H. Guo, Y.L. Liu, Y.F. Yang, S. Yang, Effects of angiotensin II intervention on MMP-2, MMP-9, TIMP-1, and collagen expression in rats with pulmonary hypertension, *Genet. Mol. Res.: Gmr.* 14 (1) (2015) 1707–1717. <http://dx.doi.org/10.4238/2015.March.6.17>.
- [50] M. Karin, Nuclear factor-kappaB in cancer development and progression, *Nature* 441 (7092) (2006) 431–436. <http://dx.doi.org/10.1038/nature04870>.
- [51] M.S. Hayden, S. Ghosh, Shared principles in NF-kappaB signaling, *Cell* 132 (3) (2008) 344–362. <http://dx.doi.org/10.1016/j.cell.2008.01.020>.
- [52] T. Xu, Z. Zhang, T. Liu, W. Zhang, J. Liu, W. Wang, J. Wang, Salusin-beta contributes to vascular inflammation associated with pulmonary arterial hypertension in rats, *J. Thorac. Cardiovasc. Surg.* 152 (4) (2016) 1177–1187. <http://dx.doi.org/10.1016/j.jtcvs.2016.05.056>.
- [53] S. Roychoudhury, S.K. Ghosh, T. Chakraborti, S. Chakraborti, H2O2-induced lipid peroxidation in mitochondria of pulmonary vascular smooth muscle tissue and its modification by DFO, DMTU and DIDS, *Indian J. Exp. Biol.* 34 (12) (1996) 1220–1223.
- [54] Y. Wang, M. Li, Y. Xu, N. He, L. Leng, Z. Li, Tumor necrosis factor-alpha regulates matrix metalloproteinase-2 expression and cell migration via ERK pathway in rat glomerular mesangial cells, *Cell Biol. Int.* 38 (9) (2014) 1060–1068. <http://dx.doi.org/10.1002/cbin.10298>.
- [55] M.Z. Arun, B. Reel, G.B. Sala-Newby, M. Bond, A. Tsaousi, P. Maskell, A.C. Newby, Zoledronate upregulates MMP-9 and -13 in rat vascular smooth muscle cells by inducing oxidative stress, *Drug Des., Dev. Ther.* 10 (2016) 1453–1460. <http://dx.doi.org/10.2147/DDDT.S103124>.
- [56] B. Yoval-Sanchez, J.S. Rodriguez-Zavala, Differences in susceptibility to inactivation of human aldehyde dehydrogenases by lipid peroxidation byproducts, *Chem. Res. Toxicol.* 25 (3) (2012) 722–729. <http://dx.doi.org/10.1021/tx2005184>.
- [57] J.A. Doorn, T.D. Hurley, D.R. Petersen, Inhibition of human mitochondrial aldehyde dehydrogenase by 4-hydroxynon-2-enal and 4-oxonon-2-enal, *Chem. Res. Toxicol.* 19 (1) (2006) 102–110. <http://dx.doi.org/10.1021/tx0501839>.
- [58] X. Liu, X. Sun, H. Liao, Z. Dong, J. Zhao, H. Zhu, P. Wang, L. Shen, L. Xu, X. Ma, C. Shen, F. Fan, C. Wang, K. Hu, Y. Zou, J. Ge, J. Ren, A. Sun, Mitochondrial aldehyde dehydrogenase 2 regulates revascularization in chronic, Arterioscler., Thromb., Vasc. Biol. 35 (10) (2015) 2196–2206. <http://dx.doi.org/10.1161/ATVBAHA.115.306012>.
- [59] L.L. Zhang, Y.Q. Wang, B. Fu, S.L. Zhao, Y. Kui, Aldehyde dehydrogenase 2 (ALDH2) polymorphism gene and coronary artery disease risk: a meta-analysis, *Genet. Mol. Res.: GMR* 14 (4) (2015) 18503–18514. <http://dx.doi.org/10.4238/2015.December.23.38>.
- [60] X.E. Lang, X. Wang, K.R. Zhang, J.Y. Lv, J.H. Jin, Q.S. Li, Isoflurane preconditioning confers cardioprotection by activation of ALDH2, *PLoS One* 8 (2) (2013) e52469. <http://dx.doi.org/10.1371/journal.pone.0052469>.
- [61] Y. Guo, W. Yu, D. Sun, J. Wang, C. Li, R. Zhang, S.A. Babcock, Y. Li, M. Liu, M. Ma, M. Shen, C. Zeng, N. Li, W. He, Q. Zou, Y. Zhang, H. Wang, A novel protective mechanism for mitochondrial aldehyde dehydrogenase (ALDH2) in type i diabetes-induced cardiac dysfunction: role of AMPK-regulated autophagy, *Biochim. Biophys. Acta* 1852 (2) (2015) 319–331. <http://dx.doi.org/10.1016/j.bbadis.2014.05.017>.
- [62] F. Guo, Y. Xing, Z. Zhou, Y. Dou, J. Tang, C. Gao, J. Huan, Guanine-nucleotide exchange factor H1 mediates lipopolysaccharide-induced interleukin 6 and tumor necrosis factor alpha expression in endothelial cells via activation of nuclear factor kappaB, *Shock* 37 (5) (2012) 531–538. <http://dx.doi.org/10.1097/SHK.0b013e31824caa96>.
- [63] M. Beretta, G. Wolkart, M. Scherthaner, M. Griesberger, R. Neubauer, K. Schmidt, M. Sacherer, F.R. Heinzel, S.D. Kohlwein, B. Mayer, Vascular bioactivation of nitroglycerin is catalyzed by cytosolic aldehyde dehydrogenase-2, *Circ. Res.* 110 (3) (2012) 385–393. <http://dx.doi.org/10.1161/CIRCRESAHA.111.245837>.
- [64] Y. Duan, Y. Gao, J. Zhang, Y. Chen, Y. Jiang, J. Ji, J. Zhang, X. Chen, Q. Yang, L. Su, J. Zhang, B. Liu, Z. Zhu, L. Wang, Y. Yu, Mitochondrial aldehyde dehydrogenase 2 protects gastric mucosa cells against DNA damage caused by oxidative stress, *Free Radic. Biol. Med.* 93 (2016) 165–176. <http://dx.doi.org/10.1016/j.freeradbiomed.2016.02.001>.
- [65] W. Ge, M. Yuan, A.F. Ceylan, X. Wang, J. Ren, Mitochondrial aldehyde dehydrogenase protects against doxorubicin cardiotoxicity through a transient receptor potential channel vanilloid 1-mediated mechanism, *Biochim. Biophys. Acta* 1862 (4) (2016) 622–634. <http://dx.doi.org/10.1016/j.bbadis.2015.12.014>.